13th World Conference on Earthquake Engineering
Vancouver, B.C., Canada
August 1-6, 2004
Paper No. 1550

RESIDUAL DISPLACEMENT AND POST EARTHQUAKE CAPACITY OF HIGHWAY BRIDGES

Kevin MACKIE[1]
Bozidar STOJADINOVIC[2]

SUMMARY

In any given earthquake event scenario, be it a first shock or an aftershock, the decision to limit traffic or to completely close a bridge in a highway network system hinges primarily on reconnaissance data on visible damage to the bridge. A more quantitative and systematic method for decision making by engineers, owners, and operators alike involves determination of the loss in the bridge load carrying capacity.

In a performance-based earthquake engineering context, the loss of load carrying capacity of a bridge can be described as a earthquake demand parameter. In previously formulated probabilistic seismic demand models, this demand parameter was predicted by a measure descriptive of the earthquake intensity. This method, however, is not the most accurate approach of predicting loss of load carrying capacity. It has been shown that post-earthquake residual displacement is a better proxy for capacity loss than measures of earthquake intensity. The initial load carrying capacity is defined in terms of a static pushover analysis. A comparison of loss in load carrying capacity is made between time history analysis of first shocks and aftershocks, and static analysis including residual displacements and degradation of material stiffness. These demand models are then integrated with estimates of capacity or damage in order to produce traditional fragility curves.

This paper focuses on the deterioration of bridge load carrying capacity, for both lateral and vertical loads, on reinforced concrete highway bridges of single bent configuration in California. Four methods are proposed to derive damage fragility surfaces. Such damage fragilities relate the probability of exceeding a prescribed damage limit state (loss of load carrying capacity), given a measure of earthquake intensity. Probabilistic demand and damage models are developed for each of the four methods and presented in a format compatible with the Pacific Earthquake Engineering Research Center's performance-based design probabilistic framework. Method D, that utilizes maximum and residual displacement models, produces the best prediction of load capacity loss. Finally, a simplified method for prediction of post-earthquake residual load carrying capacity is also presented.

[1] PhD candidate, University of California Berkeley, USA. Email: mackie@ce.berkeley.edu
[2] Associate Professor, University of California Berkeley, USA. Email: boza@ce.berkeley.edu

INTRODUCTION

In the context of evaluating the seismic hazard exposure of an urban region and consequences an earthquake may have on densely populated urban areas; it is necessary to evaluate the performance of bridges in a specified hazard environment. Performance must be defined in terms of discrete or continuous measures that have realistic decision-making or socio-economic implications. The PEER (Pacific Earthquake Engineering Research Center) probabilistic Performance-Based Earthquake Engineering (PBEE) framework [1] is one methodology for the complete performance-based design or evaluation problem. It allows for a consistent probabilistic treatment of loss through de-aggregated models.

The PEER framework defines such a loss modeling measure as a Decision Variable (DV). As applied to highway bridges, there are two types of DVs. First, a bridge functional DV may be understood as the post-earthquake operational state of the bridge. This implies a graded system of criteria involving lane closures, reduction in traffic volume, or complete bridge closure that are useful for traffic network modeling. Second, a bridge repair DV is the time (cost) of bridge repair and restoration. This DV is triggered only if the bridge function DV crosses the repair threshold. Therefore, the total societal cost for a given earthquake scenario is the sum of the indirect (or operational) costs from the loss of function, and the direct costs to restore previous functionality. This is particularly relevant in the case of a highway network system as the indirect losses to an urban area might greatly exceed the direct losses.

However, to arrive at a probabilistic model that relates measures of earthquake intensity (IM or Intensity Measure) to probabilities of exceeding specified threshold DV values, intermediate measures and resulting models must first be defined. The decision states of the bridge will be parameterized in terms of damage measures (DM). The DMs required for evaluation of the two DVs defined above must be realistic. Realistic DMs address relevant damage states that can be related to dollar losses, function losses, or collapse, and include treatment of bridge system or component damage depending on the DV of interest. At the bridge system level, it is possible to obtain DM data from structural reliability models of specific highway bridges. Functional DM models involving loss of lateral and vertical load carrying capacity can be generated. Resulting DVs lend themselves to evaluation of traffic capacity and loading for an earthquake scenario. Subsequently, the damage models need to be coupled to structural demands using Probabilistic Seismic Demand Models (PSDM). Structural demand models relate the IMs to measures of structural response, or Engineering Demand Parameters (EDP).

Further insight into post-earthquake decision-making may be gained from the introduction of the probability of collapse during aftershocks. Barring collapse, the subsequent decrease in performance as compared to the initial performance goals may also be of interest. Aftershock residual capacity can be seen as another method of determining post-earthquake capacity such as the lateral load carrying capacity described above.

In previous PEER and Caltrans meetings [2], several bridge system level outcomes have been discussed. The system variables all relate to a graded system of bridge performance levels such those in AASHTO [3]. These are discrete tables with traditional language such as "immediately operational", "emergency traffic only", and "closed." The goal is to provide a rational criterion for selection of these performance levels. Currently, Caltrans decision makers use information from post-earthquake bridge inspections to determine whether certain transportation links remain open or closed. Decisions are made based on observed damage to the roadway, settlement, permanent deformation, cracking, fracture, and buckling. Largely subjective decisions are then made on whether the bridge can support live load, and whether it has enough lateral load capacity to withstand an aftershock. This information may be supplemented by pictorial databases relating types of observable damage with expected post-earthquake performance.

However, on a more rational basis, loss in the vertical and lateral load carrying capacity can better be used for separating bridges into different performance levels. These need not only be open and closed, and can include a continuous distribution based on traffic load carrying capacity relative to the initial or design value. Therefore, the bridge-level DMs to be developed must include information on the degradation of a bridge's load carrying capacity. The issue of structural safety also arises when considering subsequent shocks. The decision to assign a damaged bridge to a certain performance level may be more influenced by this safety factor, rather than it's immediate load carrying capacity.

PROBABILISTIC MODELS

In order to develop a probabilistic assessment of the loss of load carrying capacity, it is necessary to develop rigorous interim models. Specifically, these interim models correspond directly to those of the PEER methodology [1]; demand models and damage models. As mentioned in the PEER methodology summary, demand models relate structural response measures (EDP) to earthquake intensity measures (IM). Damage models then attempt to relate the EDPs to levels of damage (DM). The demand and damage models used in the remainder of this paper are presented in this section. Hazard enters into the procedure only as measures of earthquake intensity (IM). Probabilistic Seismic Hazard Analysis and the resulting annual probabilities of exceeding each interim variable in the PEER framework are simple extensions of the models presented in this paper. The loss modeling issue and transition from DMs to DVs are addressed briefly in the Conclusion.

All of the PBEE models in this paper are developed specifically for reinforced concrete highway overpass bridges in California. These are designed according to the California Department of Transportations' (Caltrans) Seismic Design Criteria [4] with ductile failure modes. The bridge under consideration in this study is the two-equal-span, single bent, single column per bent bridge detailed in Mackie [5]. Several of the PSDMs are shown with a selection of four different design parameter values. These correspond to four different bridge designs with varying span (L) to height (H) ratios. The span is held constant throughout; therefore a higher L/H ratio implies shorter columns and a stiffer structure. All of the structural analysis and response simulations were performed using OpenSees (http://opensees.berkeley.edu/), the PEER finite element analysis platform.

Probabilistic Seismic Demand Model

Numerous PSDMs, specific to this bridge, exist already for component and global level EDPs [6]. A large amount of research exists on the selection of an optimal IM to better predict the EDP chosen [eg. 6, 7]. In this study, only the first mode spectral displacement, $Sd(T_1)$, and peak ground displacement are used (PGD). The global EDPs of interest in this study are maximum longitudinal drift ratio (or maximum longitudinal displacement) and permanent residual displacement. Both EDPs are measured at the top of the column, not at the deck-abutment interface. The resulting PSDMs using $Sd(T_1)$ and the two global EDPs are shown in Figure 1 and Figure 2, respectively.

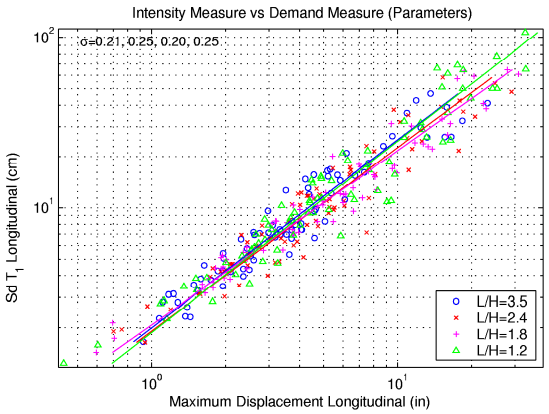

Figure 1 - PSDM $Sd(T_1)$-u_{max} long.

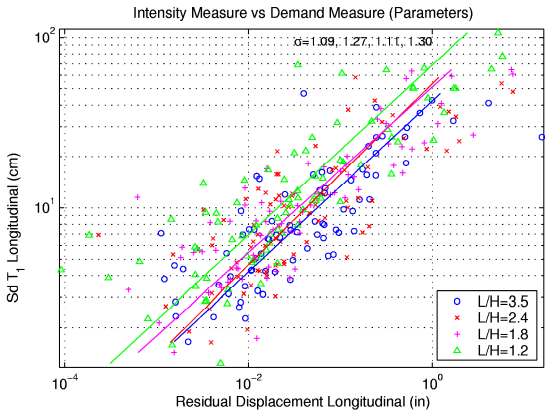

Figure 2 - PSDM $Sd(T_1)$-u_{res} long.

The dispersions associated with each PSDM are shown in the upper left of the plot window. These indicate the efficiency of the demand models and can be used to evaluate different PSDM choices. The dispersions are calculated relative to a linear fit to the median in log space [8]. The $Sd(T_1)$-u_{max} PSDM is a highly efficient model (dispersion on the order of 0.25), as evident in Figure 1. This is not true of the PSDM involving residual displacement where dispersion is on the order of 1.25. Both of the global EDP PSDMs can be described by a single relation in the form of Equation 1. The dispersions in Figure 2 clearly indicate that $Sd(T_1)$ is not a good predictor of residual displacement. This is in large part due to the fact that residual displacement is less a function of traditional intensity, but rather of inelastic excursions and the finite element model utilized. Improving this prediction is a topic of discussion in this paper.

$$\hat{EDP} = a(IM)^b \tag{1}$$

Another category of EDPs not previously addressed in Mackie [6] is the functional EDP. These are more explicitly related to the bridge structural system performance. Specifically, the functional EDPs considered in this study are the post-earthquake residual load carrying capacity of the bridge. The residual load carrying capacity can be determined in both lateral directions (longitudinal and transverse), as well as the vertical direction. The value of the EDP is determined from a static nonlinear pushover of the structure in the lateral directions and a pushunder in the vertical direction. A pushunder is analogous to a pushover, except the load is applied vertically downward, and the vertical displacement is monitored. Results of a pushunder may be interpreted in terms of a gravity load safety factor [9]. These functional EDPs become measures of demand as they are executed after a dynamic time-history analysis. Therefore, the residual load carrying capacity of a bridge would be expected to degrade as the intensity of an earthquake event increases. To facilitate simpler demand model computations, the EDP is defined relative to the load carrying capacity at IM = 0 (Equation 2). The functional demand parameter is thus termed the loss of load carrying capacity (in force space), but should not be confused with the variability inherent in the capacity of the bridge system in the absence of earthquake loading. The resulting PSDMs, once again using $Sd(T_1)$, for the loss of longitudinal and vertical load carrying capacities are shown in Figure 3 and Figure 4, respectively.

$$EDP = EDP_{IM=0} - EDP_i \tag{2}$$

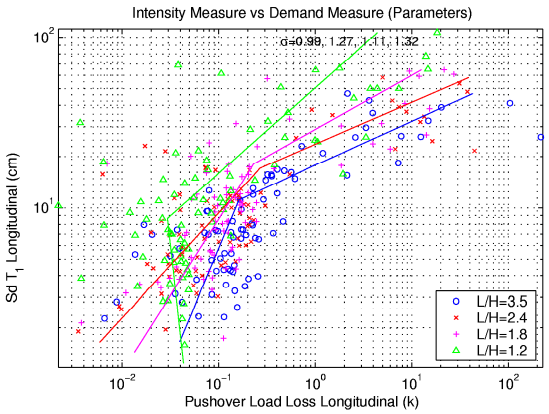

Figure 3 – PSDM $Sd(T_1)$-Capacity loss long.

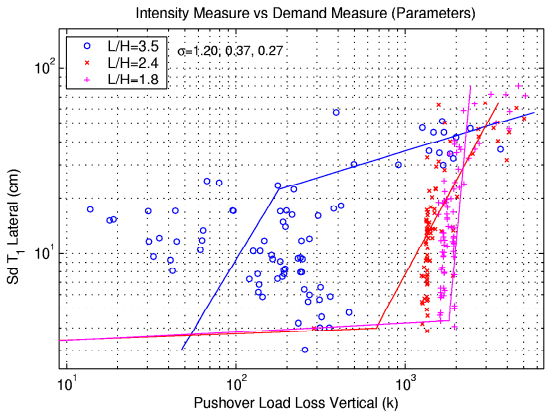

Figure 4 - PSDM $Sd(T_1)$-Capacity loss vert.

Unlike Figure 1 and Figure 2, these functional EDPs cannot be described effectively by a single linear fit (in log space). They exhibit two regimes of behavior that require separate fitting. The low intensity response of bridges is primarily linear, hence there is little or no degradation in the residual load carrying capacity. This regime is shown in Figure 3 as the vertical lines (in linear space) at small IM values. The second regime defines the range of intensities that damage the bridge structure and decrease its ability to carrying post-earthquake loads according to Equation 1. The vertical axis on Figure 4 is a geometric combination of intensities in the longitudinal and transverse directions, and does not include a spectral component in the vertical direction. However, to maintain commonality with the fragility formulation, only the lateral IMs are included. As seen by the large scatter; however, the lateral intensities may not be the best predictors of the residual vertical load capacity.

The wide amount of scatter in the degrading regime lowers the confidence in using these demand models directly, as the selection of the median fit is highly uncertain. Not only is confidence in the median low, but there are also large dispersion values associated with the model fit. Therefore, this paper focuses on methods to improve the prediction of capacity loss through reduction in model uncertainty.

Probabilistic Seismic Demand Model for Aftershocks

The same methodology applied to the generation of PSDMs for first shock earthquake scenarios can be applied to aftershocks. For the purposes of this study, the same PSDA cloud method as described in Mackie [5] was employed to develop PSDMs for aftershocks. The only extension involves the selection of bins, aftershocks bins, and the sequence of first-shock and aftershock events. To maintain continuity, the same first-shock bins were employed. After each first shock, the structure was allowed to come to rest before randomly selecting an aftershock record from one of five different aftershock bins. A single bin of specific recorded aftershock time histories were selected from the PEER ground motion catalog (http://peer.berkeley.edu/smcat/). These were scaled up by a factor of two in order to ensure damage in the structure occurred. The remaining four bins were identical to the first-shock bins, but with intensity scaled by a factor of a half. Each first-shock bin was paired with each aftershock bin, creating a total of 20 bins for analysis. Therefore, for every structure, the required computations increased by a factor of 5. For this reason, only the structure with a L/H ratio of 2.4 is pursued in the aftershock scenarios.

The IM of the first-shock is maintained throughout the aftershock analysis and used in the prediction of the ultimate EDP value. The first shock (FS) IM is termed $IM_{FS} = IM_1$, while the aftershock (AS) IM is termed $IM_{AS} = IM_2$. The same two global EDP measures used in Figure 1 and Figure 2 are presented here for the aftershock scenario in Figure 5 and Figure 6, respectively. As in the case of the first-shock PSDMs, a linear fit was made to the data (now a plane in log space). The resulting dispersions are 0.27

for Figure 5 and 1.33 for Figure 6. Of note from these PSDMs is the dependence of u_{max} almost exclusively on IM_2. On the contrary, u_{res} is a function of both IM_1 and IM_2.

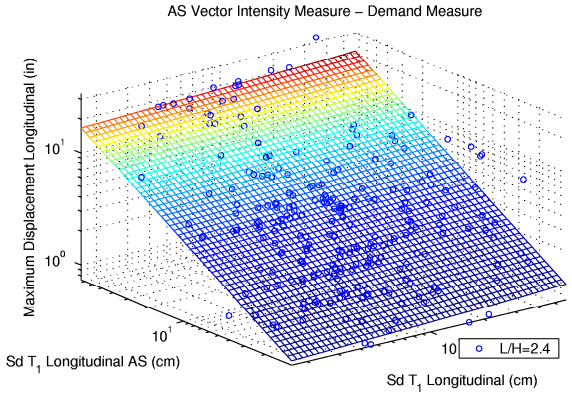

Figure 5 - Aftershock PSDM $Sd(T_1)$-u_{max} long.

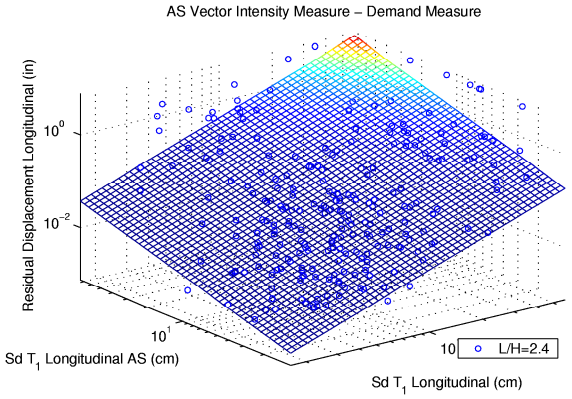

Figure 6 - Aftershock PSDM $Sd(T_1)$-u_{res} long.

Probabilistic Damage Model

Given the bridge system functionality implied by the EDP (loss of load carrying capacity), it is necessary to extend the EDPs to DMs at the bridge level as well. The corresponding DM is the loss of lateral or vertical load carrying capacity (as a percent of the original). This DM value is produced by introducing a prediction of pre-earthquake load carrying capacity and then comparing to the residual load carrying capacity in a demand/capacity evaluation. The pre-earthquake load carrying capacity is determined using a nonlinear static pushover or pushunder in the same manner as the demand model. However, to incorporate uncertainty in the pre-earthquake capacity, a structural reliability approach was adopted.

Reliability tools incorporated into OpenSees by Haukaas [10] were used to develop damage models that relate the probability of exceeding a DM level, given the demand (EDP). A total of ten random variables were used in the bridge model to determine the distribution of response. These random variables include the uncertainty in materials, geometry, soil stiffness, and dead loading. The structural reliability tools then attempt to estimate the probability of exceeding values of specified limit state functions. The limit state function is usually denoted as $g(\mathbf{x})$, where $\mathbf{x}$ is the vector of random variables considered in the problem, and $g(\mathbf{x}) \leq 0$ usually defines the failure domain (eg. when demand exceeds capacity). The limit state function (Equation 3) was defined in terms of the pre-earthquake lateral load carrying capacity (P_{DM}) at different levels of demand (EDP_i). The damage limit state is the force at the location on the pushover curve where 1-dm^{LS} (%) of ultimate load exists. The probability of failure was estimated using FORM (first order reliability method) analysis at each level of demand.

$$g(\mathbf{x}) = P_{@\,DM=dm^{LS},long}(\mathbf{x}) - EDP_i \tag{3}$$

For the limit state DM = 0 (no loss of load carrying capacity), the results of FORM analysis are shown for longitudinal load and vertical load in Figure 7 and Figure 8, respectively. The estimated PDF for the damage model is shown in the bottom pane of each plot.

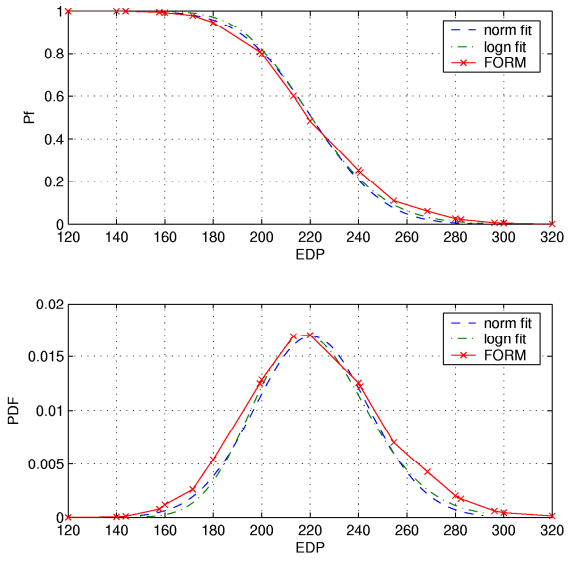

Figure 7 - Damage model longitudinal

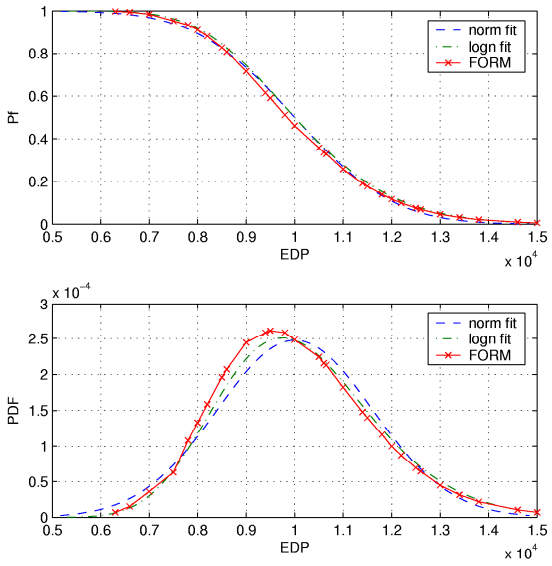

Figure 8 - Damage model vertical

Each point on the CDF curves corresponds to a FORM analysis at a given EDP level (EDP_i). In order to facilitate computations with the damage models shown, normal and lognormal distributions are fit to the data points. The lognormal fit is used in subsequent damage models rather than the first order approximation points. Similar damage models were obtained for other values of dm^{LS}, or were obtained by scaling the lognormal distributions according to a constant coefficient of variation.

Damage Fragility

The ultimate goal of generating individual demand and damage models is to combine them for a meaningful result. One method of visualizing damage probability is the fragility curve. In this paper, only damage fragilities are developed (interim demand fragilities can also be produced). The formulation for damage fragility using the PEER framework is shown in Equation 4.

$$P\left[DM < dm^{LS} \middle| IM = im\right] = \int_{edp} P\left[DM < dm^{LS} \middle| EDP = edp\right] dP\left[EDP < edp \middle| IM = im\right] dedp \qquad (4)$$

The first term is the CDF obtained directly from the reliability-based damage models. The second term is a PDF of response (EDP) at a given IM level. The resulting curve for each damage limit state (dm^{LS}) shows the probability of exceeding the limit state given a range of intensities (IM).

POST-EARTHQUAKE CAPACITY METHODS

While it is possible to directly assess the post-earthquake capacity using the traditional PEER formulation, the large uncertainty in this method facilitates development of better methods of prediction. The alternate formulations are also important when determining the aftershock load carrying capacity of the bridge. The large amount of computation required to develop post-earthquake residual load carrying capacity curves is multiplied when developing curves for aftershock scenarios. In this case, the data required for the direct method may not be available. The direct method is addressed as Method A below, followed by three options for better predicting damage fragility in terms of loss of load carrying capacity.

Method A – Direct Method

This method is a specific application of Equation 4 to the PSDMs involving residual load carrying capacity shown in Figure 3 and Figure 4. The resulting damage fragilities showing the loss of lateral and vertical load carrying capacity are shown in Figure 9 and Figure 10, respectively. In order to reduce the scope of this paper, only the vertical load carrying results are presented from this point on.

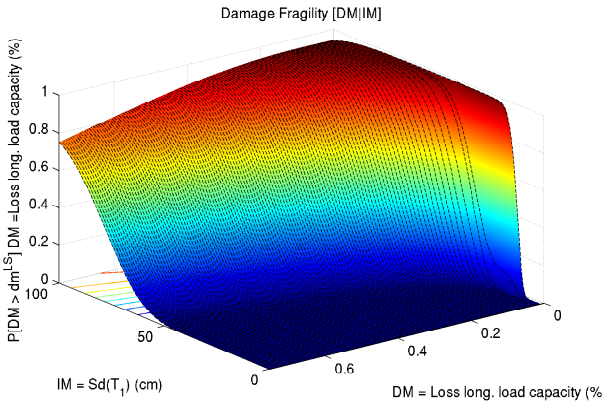

Figure 9 - Method A longitudinal

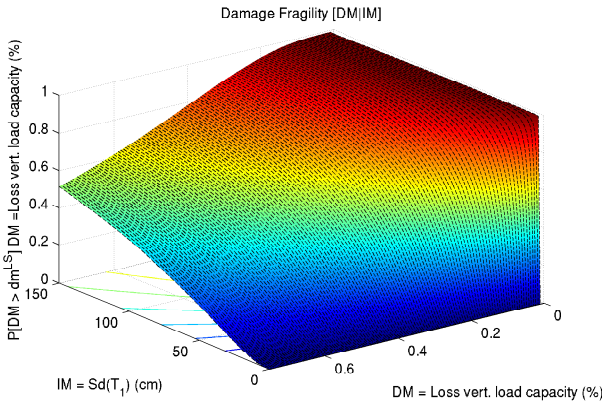

Figure 10 - Method A vertical

While Method A appears to generate effective results, the selection of the median PSDM for the first-shock post-earthquake scenario is highly uncertain, especially at higher intensities. The dispersion value used to generate the PSDMs is artificially low due to the lack of dispersion in the linear regime of bridge behavior. The difference in low intensity behavior becomes apparent when comparing all of the subsequent methods. Nonetheless, the dispersion in the nonlinear range of response is large, creating an inordinately long tail of the PDF. The magnitude of the IM axis is curtailed at $Sd(T_1)$ = 150 cm (corresponds to a spectral acceleration of 2.4g). The net result is a probability of 1 not being obtained for all but the smallest DM values. Method A is compared with the other methods in the Results section.

Method B – MDOF Residual Displacement Method

This method introduces the importance of the correlation between post-earthquake capacity and residual displacement. An intermediate variable, post-earthquake residual displacement (u_{res}), is introduced between the EDP and IM variables. The resulting formulation is shown in Equation 5. This method is beneficial because the relationship between residual displacement and earthquake intensity was already developed during previous PSDM studies [6]. However, there is large uncertainty in predicting residual displacement, especially given a spectral IM such as *Sd* or *Sa*. A better IM for predicting u_{res} for this bridge is *PGD*. But to maintain consistency between examples, $Sd(T_1)$ is used.

$$P[loss] = \iint P[damage] \cdot dP[EDP < edp \mid EDP = u_{res}]\, dP[EDP < u_{res} \mid IM = im]\, dedp \cdot du_{res} \quad (5)$$

where $$P[loss] = P[DM < dm^{LS} \mid IM = im] \quad (6)$$

$$P[damage] = P[DM < dm^{LS} \mid EDP = edp] \quad (7)$$

In order to utilize this method, a relationship between residual displacement and loss of capacity needs to be developed. This is shown in Figure 11 for the vertical direction. The loss of capacity is due to not only the degradation of stiffness and strength, but also the presence of P-Δ effects for large residual displacements. A linear fit was made to the residual displacement values larger than 2 inches and extended to the origin in order to provide a smooth transition to earthquake intensities. This prevents a jump in load carrying capacity loss around zero intensity. The resulting fragility surface showing the

probability of exceeding different levels of vertical load carrying capacity loss is shown in Figure 12. Due to the large intensity required to obtain large residual displacements (Figure 2), the probabilities of exceeding large load losses are small. Not only this, but the method suffers from the same large dispersion problem as Method A, this time due to the uncertainty in the residual displacement PSDM. Once again, all methods are compared in the Results section.

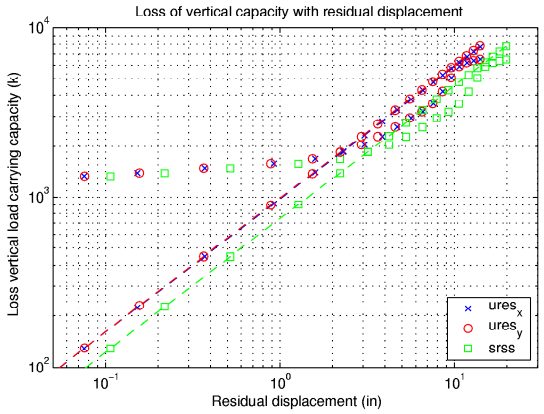

Figure 11 - u_{res} vs Capacity loss vertical

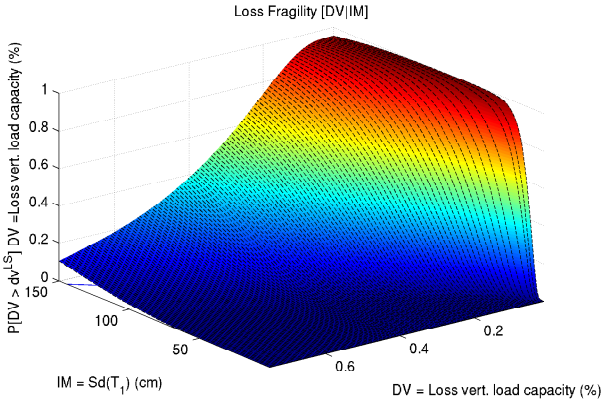

Figure 12 - Method B vertical

Method C – SDOF Residual Displacement Method

Method B and method C utilize the same formulation (Equation 5) involving residual displacements. The difference with this method is the assumption that residual displacements can be derived using a residual displacement spectrum from equivalent single-degree-of-freedom (SDOF) systems. The large uncertainty in the PSDM term in Method B motivated a better method for predicting u_{res}. Residual displacement spectra have been examined before by Kawashima [11]. Sensitivity to earthquake intensity was only examined for measures such as magnitude and distance. In this study, the residual displacement of single-degree-of-freedom oscillators was regressed against arbitrary measures of earthquake intensity (IM). This makes the procedure analogous to PSDA for more complex structures.

The inelastic SDOF oscillator employed in this study had the same initial elastic period of the bridge (T_1). The entire spectrum was not generated for each ground motion, ie, only the residual displacement at T_1 was calculated. The inelastic oscillator's yield strength was taken from the nonlinear pushover of the bridge in the longitudinal and transverse directions. Previous analyses [6] had shown the R factor for this bridge configuration with respect to the USGS 2% in 50 year hazard spectrum was 3.6 for T_1 (transverse direction) and 4.0 for T_2 (longitudinal direction). A value of R = 4 and a hardening ratio of 1.5% for the bilinear SDOF oscillator were therefore assumed. The resulting residual displacements can be plotted in a manner consistent with PSDMs, as shown in Figure 13.

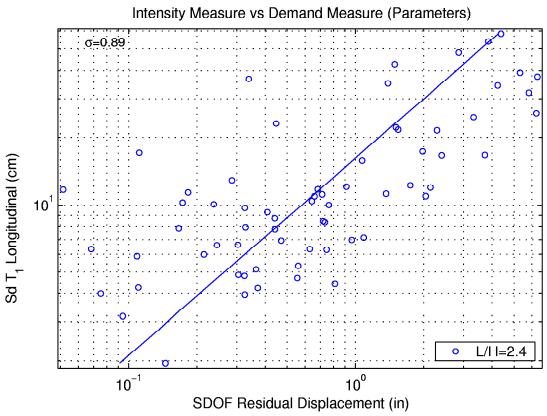

Figure 13 - SDOF PSDM $Sd(T_1)$-u_{res}

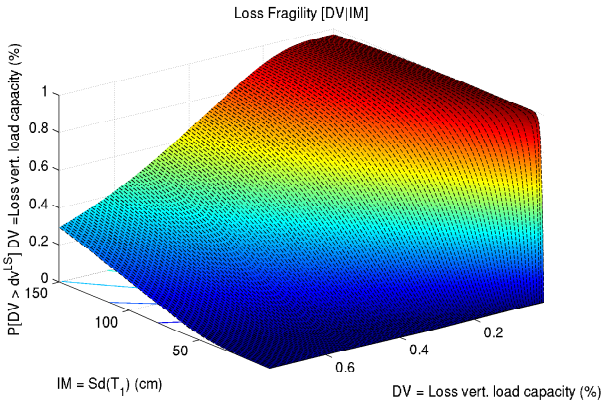

Figure 14 - Method C vertical

The intent of Method C was to reduce to dispersion in the PSDM term used in Method B. As evidenced in Figure 13, SDOF oscillators also have a large amount of uncertainty in predicting residual displacements (with *Sd*). Therefore, the results are similar for Methods B and C, with the slight discrepancy arising from the residual displacement values predicted and the resulting loss in capacity from Figure 11. The advantage of this method is avoiding PSDA on a complex bridge structure and using SDOF data instead. The disadvantage of using this method is the selection of T_1 for the SDOF oscillator. More complex finite element models capture the softening of the fundamental period with accumulation of damage (Method B), but the period of the SDOF system is fixed.

Method D – EDP Correlation Method

This method attempts to eliminate the dependence on interim models that have low efficiency. In order to accomplish this, the maximum displacement is introduced and correlated with residual displacement. The PSDM involving maximum displacement (or drift ratio) is known to be highly efficient [6]. By introducing yet another interim variable, u_{max}, it is attempted to improve the prediction of vertical loss in load carrying capacity. The form of the framing equation becomes Equation 8.

$$P[loss] = \iiint P[damage]dP[EDP < edp \mid u_{res}]dP[u_{res} \mid u_{\max}]dP[u_{\max} \mid im]dedp \cdot du_{res} \cdot du_{\max} \qquad (8)$$

The name of the random variable each term is conditioned on has been omitted to save space, but can be inferred from the context.

The only relationship not yet formulated in this method is that between maximum displacement and residual displacement. This data can also be obtained from previous PSDM studies for this bridge. Even though the residual displacement is plotted on the ordinate, the lognormal fits are made with maximum displacement as the dependent variable (this is opposite to the other PSDMs presented). The resulting plots for the longitudinal and transverse directions are shown in Figure 15 and Figure 16, respectively.

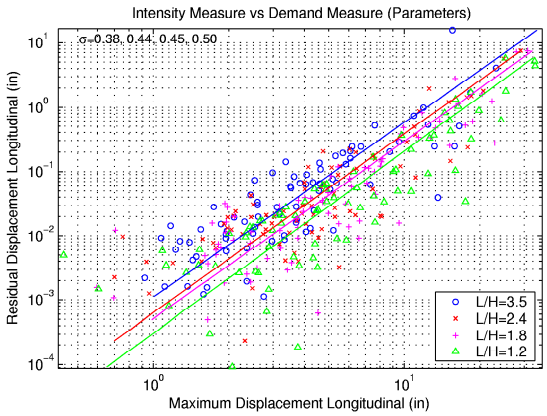

Figure 15 - u_{max} vs u_{res} longitudinal

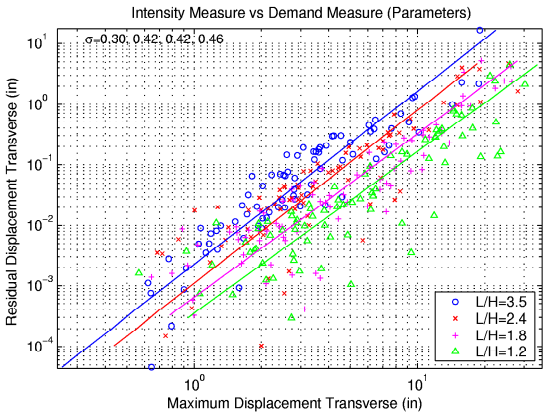

Figure 16 - u_{max} vs u_{res} transverse

Integrating all of the interim models together provides a final form for the loss of vertical capacity (Figure 17). The form is very similar to all of the previous methods, but has the advantage of higher confidence in the results due to the lower dispersions of the interim models. However, it suffers from the number of parameters required to fully describe all the models, and the model error associated with each of these.

POST-AFTERSHOCK CAPACITY METHODS

Several of the methods above can be applied directly to the performance of highway bridges during aftershock scenarios. This is accomplished by using the PSDM planes presented in the Demand model section. Response to aftershock events can be conditioned on the intensity of the first-shock by using response functions involving both intensities. As an example in this paper, a first-shock intensity of $Sd(T_1)$ = 40 cm (corresponds to a spectral acceleration of 0.65g) was selected.

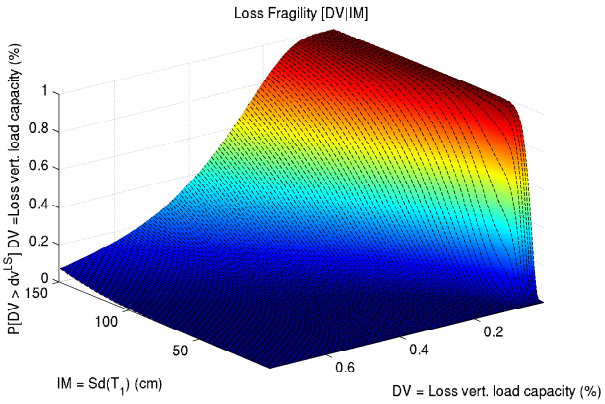

Figure 17 - Method D vertical

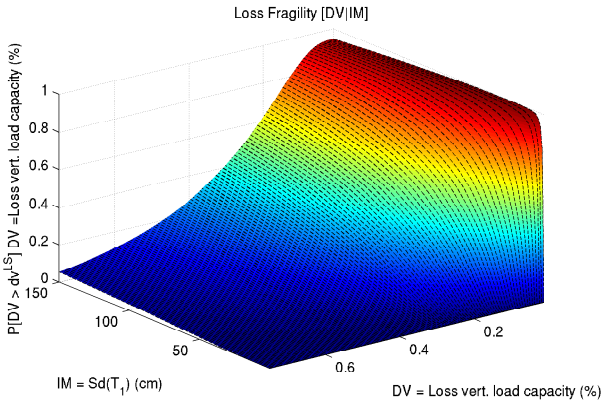

Figure 18 - Aftershock Method B vertical

Method B – MDOF Residual Displacement Method

The same methodology was applied in the aftershock scenario as for the Method B first-shock case. The third term in Equation 5 was the only modification, containing data from the aftershock PSDM conditioned on IM_1 (the first-shock intensity). The resulting fragility surface is shown in Figure 18. In this figure, the IM axis now describes the intensity of the aftershock, once again using $Sd(T_1)$. It should be noted that this may not be the best choice of IM for an aftershock scenario as the fundamental period of the structure would have shifted due to the first-shock. However, to maintain commonality between

methods, it is necessary to keep the same T_1 value. A better solution would be to determine the optimal non-structure-dependent IM for this bridge, allowing objective comparisons between arbitrary events. Structure independent IMs are discussed in Mackie [6].

A further distinction involving the response from the aftershock scenario is also required. The PSDMs of Figure 5 and Figure 6 provide a relationship between global displacement response due to an aftershock intensity IM_2, conditioned on a first-shock intensity IM_1. However, loss of load carrying capacity is obtained separately, independent of both intensities. Therefore, the vertical load carrying capacity loss surface does not describe the cumulative effect of both the first-shock and the aftershock. An estimate of the total fragility for the aftershock is made in the next section.

Method D – EDP Correlation Method

Similarly, Equation 8 was applied as for Method D in the first-shock case. The fourth term in the equation now contains data from the aftershock PSDM. The resulting fragility surface is shown in Figure 19.

RESULTS

Method Comparison

All of the proposed methods are compared here for a single limit state value of 10% loss of vertical load carrying capacity. These are now plotted as single fragility curves (Figure 20), obtained directly from the fragility surfaces in the figures above. The average of all the methods is also included for comparison. Numerous other limit state values were also investigated (25% and 50%), but the summary plots are excluded from this paper as the trends implicit in the methods are readily apparent from the $dm^{LS} = 10\%$ example. It is ostensible from Figure 20 that methods B, C, and D give different results from the single step Method A. This is to be expected given the lack of confidence in the median relationship between IM and EDP in Figure 4. In the vertical direction, Method A does not exhibit a linear regime of behavior at low intensities. This results in an immediate increase in damage, even for low intensity events. The immediate onset of damage is not realistic; the curve should be shifted to the right. Therefore, Method A gives a conservative upper bound.

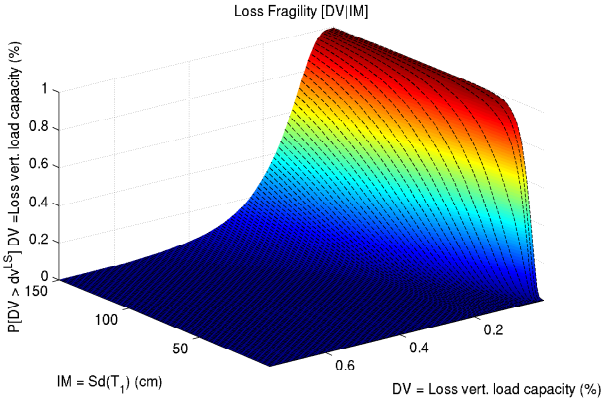

Figure 19 - Aftershock Method D vertical

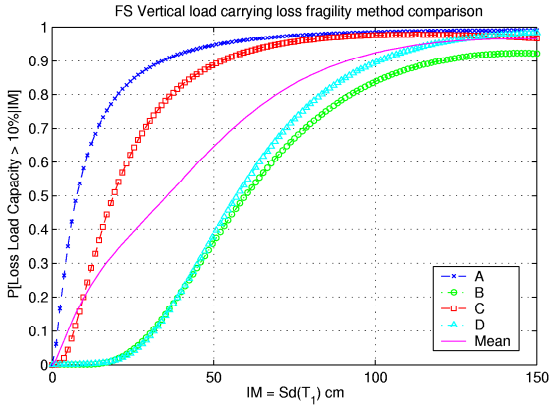

Figure 20 - First shock method comparison

Of interest when comparing the different methods is the value of the IM at the mean and the standard deviation of the fragility curve. Methods B and D have a similar mean. This would be expected given the PSDM data for all interim models came from the same finite element analysis. Method C has the same form as Method B due to it's formulation; however, the mean is shifted because the SDOF system was not modified by a modal participation factor in this analysis and does not account for more complex system

interaction. All of the methods, except D, exhibit large dispersion in the final fragility. This is due to the large uncertainty in the interim models and results in inaccurate probability tails.

Of the multiple step methods (B, C, and D), they all correctly predict a threshold intensity value, below which there is no damage. As mentioned, the SDOF mean is shifted but could be corrected based on the modal participation factor even though the problem is not strictly linear (for modal analysis). Of the individual methods, method D appears the best single method (based on dispersion) for prediction of the loss of vertical load carrying capacity.

The methods can also be compared using data from the aftershock fragilities. The two fragility curves, their average, and the average from the first-shocks alone are shown in Figure 21. To be consistent between the aftershock and first-shock methods, it was attempted to derive the aftershock fragility surface using Method A (results not shown here). Due to the large amount of computation required and the lack of a best-fit plane, Method A was shown to be a poor prediction tool when considering aftershocks.

Since residual displacement and maximum displacement are functions of the aftershock intensity (IM_2), they are not good reflectors of cumulative damage during multiple events. This is indicated by aftershock Method D closely mimicking the behavior of its first shock counterpart. However, given the first-shock probabilities from Figure 20, as well as aftershock probabilities of IM_2 conditioned on IM_1, it is possible to find the total probability by the union of the events. The independent first-shock and aftershock probabilities were assumed equal (if the events occurred individually). This total fragility curve is also shown in Figure 21 (for Method B and D), and reflects the likely probability of exceeding 10% loss in vertical load carrying capacity with an aftershock of intensity IM_2 on the abscissa. The fragility curve exceeding a value of 1 is due to the assumption that the first-shock and aftershock events can be considered independently.

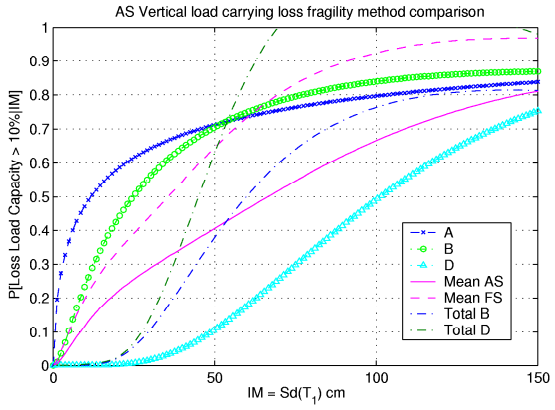

Figure 21 - Aftershock method comparison

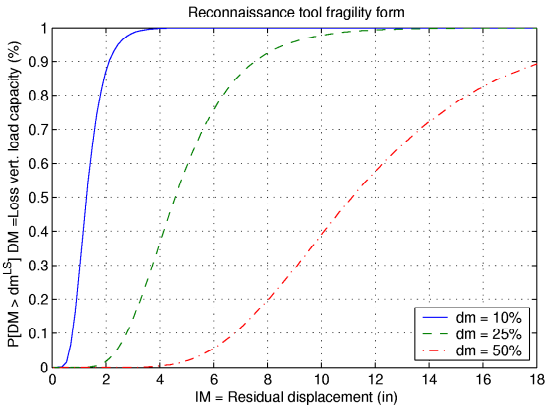

Figure 22 - u_{res} fragility tool

Simplified Reconnaissance Tool

The primary use of post-earthquake load carrying capacity is envisioned as a decision making tool for engineers and policy makers in a highway network environment. Proposed decision states based on the loss of load carrying capacity are presented in [12], and repeated here for comparison (Table 1). Using such a table, calibrated by the institution evaluating the highway bridges, and a simplified method for determining the residual load carrying capacity of a bridge, it would be possible to effect a more rational performance-based decision-making process.

Table 1 - Proposed performance levels using bridge-level DVs

Objective name	Traffic capacity remaining (volume)	Loss of lateral load carrying capacity	Loss of vertical load carrying capacity
Immediate access	100%	< 2%	< 5%
Weight restriction	75%	< 2%	< 10%
One lane open only	50%	< 5%	< 25%
Emergency access only	25%	< 20%	< 50%
Closed	0%	> 20%	> 50%

In a pre-earthquake design or emergency response analysis, it may be possible to predict earthquake intensities at individual geographically distributed sites. However, a more useful tool in the hands of a field engineer would be a rational basis for decision-making that is based on criteria that do not require the input earthquake intensity at the bridge site. While the methods in this paper are only preliminary indications that residual displacement provides a useful pathway for prediction of loss of load carrying capacity, residual displacement has long been used in practice as a means for evaluating a bridge post-earthquake. With the frameworks presented in this paper, it would be possible to develop such a tool by integrating only the first two terms of Equation 5 (Method B). The resulting formulation is shown in Equation 9.

$$P\left[DM < dm^{LS} \mid IM = u_{res}\right] = \int P\left[DM < dm^{LS} \mid EDP = edp\right] dP\left[EDP < edp \mid IM = u_{res}\right] dedp \qquad (9)$$

Using the same interim models as Method B, Equation 9 can be evaluated for different limit states of interest. Fragility curves for three limit states are plotted versus residual displacement in Figure 22. Conceptually, this simplified tool could also be generated using the first three terms of Equation 8 (from Method D) in order to reduce the dispersion.

For example, Table 1 and Figure 22 can be used to assess the post-earthquake performance of a bridge within a highway network. A rejection (acceptance) criterion for each performance objective in the table must be selected, such as a 75% probability that greater than 10% (or 25% probability that less than 10%) of the vertical load carrying capacity has been lost constitutes bridge weight restrictions. A field engineer can then assess the condition of the bridge according to its residual displacement. If the residual displacement was determined to be 2 in, then from Figure 22, the probability of exceeding a 10% loss of capacity is 0.87 and the probability of exceeding a 25% loss of capacity is 0.02. The 87% probability of exceedance surpasses the 75% threshold; therefore weight restrictions should be issued. The 2% probability of exceeding 25% loss does not exceed the next performance threshold, so no lane closures are required. The performance thresholds and acceptance criteria are merely examples, to be modified based on practitioner input.

CONCLUSIONS

This paper provides a proof of concept for more rational and quantifiable decision-making criteria for reinforced concrete highway bridges. The criteria selected to evaluate functionality of bridges after a first-shock or aftershock scenario are the loss of bridge lateral and vertical load carrying capacities. While current decisions to limit traffic or to completely close a bridge in a highway network system rely on inspection data, these can be supplemented by the use of the reconnaissance tool and a sample set of graded performance criteria proposed in this paper. The specific values of load carrying capacity loss at different performance levels remain to be finalized; however, the methods utilized in this paper can be generalized to any such values.

Four methods of obtaining the loss of load carrying capacity were investigated. The methods introduce post-earthquake residual displacement as a better proxy for capacity loss rather than measures of earthquake intensity. In order to reduce the dispersions inherent in each interim model, subsequent methods attempt to further de-aggregate the problem until more efficient models exist. In this manner, Method D was shown to be the best single method for determining vertical capacity loss, expressed in the form of a damage fragility surface. This method correlates two EDPs (maximum displacement and residual displacement) and capacity loss through a series of models obtained from Probabilistic Seismic Demand Analysis (PSDA) and finite element simulation. The methods can be also applied to aftershock post-earthquake capacity, although more work is needed on damage dependence for aftershocks.

Residual displacement gives us a prediction of loss of load carrying capacity, as desired, but it is still not the best correlation between IM and loss of capacity. Dispersions are still large and, while some are aleatory, most epistemic sources still need work. For example, there may be a bias in computing residual displacement introduced by the hysteretic model used in finite element analysis. The power of using Method B, D, or D is each interim model can be optimized to reduce dispersion. For example, a better IM predictor of residual displacement can be used to greatly enhance the overall prediction of load carrying capacity loss. Information about selection of better IMs already exists in Mackie [6].

ACKNOWLEDGEMENTS

This work was supported in part by the Earthquake Engineering Research Centers Program of the National Science Foundation under award number EEC-9701568 through the Pacific Earthquake Engineering Research Center (PEER). Any opinions, findings, and conclusions or recommendations expressed in this material are those of the author(s) and do not necessarily reflect those of the National Science Foundation.

REFERENCES

1. Cornell CA, Krawinkler H. “Progress and challenges in seismic performance assessment.” PEER Center News 2000; 3(2).
2. Porter K. Minutes from PEER/Caltrans meetings and notes. 2/27/02 and 5/14/02. Sacramento: California Department of Transportation, 2002.
3. ATC/MCEER. “Recommended LRFD guidelines for the seismic design of highway bridges.” ATC Report No. ATC-49a. Applied Technology Council and Multidisciplinary Center for Earthquake Engineering joint venture, 2001.
4. Caltrans. “Seismic Design Criteria 1.1.” Sacramento: California Department of Transportation, 1999.
5. Mackie K, Stojadinovic B. “Probabilistic seismic demand model for California highway bridges.” Journal of Bridge Engineering 2001; 6(6): 468-481.
6. Mackie K, Stojadinovic B. “Seismic demands for performance-based design of bridges.” PEER Report. Submitted for publication, 2003.
7. Cordova PP. “Development of a two-parameter seismic intensity measure and probabilistic seismic assessment procedure.” PEER Report 2000/10. Berkeley: Pacific Earthquake Engineering Research Center, University of California Berkeley, 2000:.
8. Shome N, Cornell CA. “Probabilistic seismic demand analysis of nonlinear structures.” Reliability of Marine Structures Report No. RMS-35. Stanford: Department of Civil and Environmental Engineering, Stanford University, 1999.
9. Deierlein G.
10. Haukaas T. “Finite element reliability and sensitivity analysis of hysteretic degrading structures.” PhD Dissertation, University of California Berkeley, 2003.

11. Kawashima K, MacRae GA, Hoshikuma J, Nagaya K. "Residual displacement response spectrum." Journal of Structural Engineering 1998; 124(5): 523-530.
12. Mackie K, Stojadinovic B. "Fragility curves for reinforced concrete highway overpass bridges." Proceedings of the 13th World Conference on Earthquake Engineering, Vancouver CA. Submitted for publication, 2003.